A R C H I V E S O F M E T A L L U R G Y A N D M A T E R I A L S
Volume 58 2013 Issue 2
DOI: 10.2478/amm-2013-0008

T. KVAČKAJ*, R. KOČIŠKO*, J. TIŽA*, J. BIDULSKÁ*, A. KOVÁČOVÁ*, R. BIDULSKÝ*, J. BACSÓ*, M. VLADO*

APPLICATION OF WORKABILITY TEST TO SPD PROCESSING

ZASTOSOWANIE TESTU OBRABIALNOŚCI DO INTENSYWNEGO ODKSZTAŁCENIA PLASTYCZNEGO

The aluminium alloy with chemical conception AlMgSi prepared by PM (powder metallurgy) technology was used. The experiments such as a ring and compression test, ECAR (equal channel angular rolling) for determination of friction coefficient, stress-strain curves and material workability based on analytical methods (Freudenthal, Cockcroft-Latham and normalized Cockcroft-Latham criteria) were performed. Numerical simulations of sample processed by ECAR was carried out by a software Deform 3D with focus on the description of stress, strain fields and workability criteria (Cockcroft-Latham and normalized Cockcroft-Latham). The prediction of fracture formations in a real ECAR sample during processing conditions was also done.

Keywords: compression test, powder metallurgy, fracture criteria, ECAR, Deform 3D

Stop aluminium o składzie chemicznym AlMgSi przygotowano metodą proszkową. Wykonano badania takie jak próba ściskania swobodnego pierścieni i walcowatych, ECAR (wyciskanie w kanale kątowym z walcowaniem) w celu wyznaczenia współczynnika tarcia, krzywych naprężenie-odkształcenie oraz podatności materiału na odkształcenie z użyciem metod analitycznych (kryterium Freudenthal, Cockcroft-Latham i znormalizowane Cockcroft-Latham). Symulacje numeryczne dla próbki poddawanej procesowi ECAR przeprowadzono przy pomocy oprogramowania Deform 3D z naciskiem na opis pól sił i naprężeń oraz kryteriów obrabialności (Cockcroft-Latham i znormalizowane Cockcroft-Latham). Przeprowadzono również symulację możliwości tworzenia się pęknięć w rzeczywistej próbce poddanej procesowi ECAR.

1. Introduction

The workability can be defined as an ability of a metal to achieve a certain degree of deformation during metalworking processes without creation of defects. The material workability may be described through some criteria as are brittle and ductile fracture criteria. As material fracture in bulk deformation processing usually is as ductile fracture and rarely a brittle fracture, brittle mechanism will not be discussed in present work. The fracture mechanism mainly depends on plastic deformation conditions as a state of stress, strain, strain rate and temperature. The most widely used approaches for evaluation of material workability (ductile fracture) are based on:

– evaluation of dependence only on strains using fracture forming limit diagram (FFLD)
– evaluation of dependence by mathematical description of relationship between stress and strain.

The fracture observations based on FFLD need only information about relationship between tensile and compressive strains. Mathematical equations based on relationship between stress and strain describing ductile fractures are called workability criteria.

Workability criteria are commonly used in a simplified form considering room temperature, state of stress and strain only. Those criteria are based on integral functions of stress – strain states. The authors Atkins and Mai [1] showed that all stress-strain criteria of ductile fracture are based on Freudenthal's critical plastic work per unit of volume [2]. The Freudenthal's equation has a form:

$$\int_0^{\bar{\varepsilon}_f} \bar{\sigma} \cdot d\bar{\varepsilon} = C_1 \tag{1}$$

where:

$\bar{\sigma} \equiv \sigma_{ef}$ [MPa] – effective stress according to the von Mises
$\bar{\varepsilon} \equiv \varepsilon_{ef}$ [-] – effective strain
$\bar{\varepsilon}_f \equiv \varepsilon_{ef,f}$ [-] – effective strain in fracture
ε_i [-] – principal strains (i=1,2,3)
C_1 [MPa] – material constant (the threshold value of the criterion at the instant of fracture initiation).

According to the von Mises, the effective stress is given as follows:

$$\bar{\sigma} = \frac{1}{\sqrt{2}} \cdot \sqrt{(\sigma_1 - \sigma_2)^2 + (\sigma_2 - \sigma_3)^2 + (\sigma_1 - \sigma_3)^2} \tag{2}$$

* DEPARTMENT OF METALS FORMING, FACULTY OF METALLURGY, TECHNICAL UNIVERSITY OF KOŠICE, SLOVAKIA

According to the von Mises, the effective plastic strain increment in a simplified form is given as follows:

$$d\bar{\varepsilon} = \sqrt{\frac{2}{3}} \cdot \sqrt{d\varepsilon_1^2 + d\varepsilon_2^2 + d\varepsilon_3^2} \tag{3}$$

According to the von Mises, the total effective plastic strain is given as follows:

$$\bar{\varepsilon} = \sqrt{\frac{2}{3}} \cdot \sqrt{\varepsilon_1^2 + \varepsilon_2^2 + \varepsilon_3^2} \tag{4}$$

The relationship between effective stresses and strains in a fracture point described by Freudenthal's fracture model should be considered with power hardening Ludwig – Hollomon's dependence $\bar{\sigma}_f = \bar{\sigma}(\bar{\varepsilon}_f)$ which will be defined in a fracture point as follows:

$$\bar{\sigma}_f = K \cdot \bar{\varepsilon}_f^n \tag{5}$$

and Eq.(1) can be in a form:

$$\int_0^{\bar{\varepsilon}_f} \bar{\sigma} \cdot d\bar{\varepsilon} = \int_0^{\bar{\varepsilon}_f} \bar{\sigma}(\bar{\varepsilon}) \cdot d\bar{\varepsilon} = \int_0^{\bar{\varepsilon}_f} K \cdot \bar{\varepsilon}^n \cdot d\bar{\varepsilon} = K \cdot \frac{\bar{\varepsilon}_f^{n+1}}{n+1} = C_1 \tag{6}$$

where:

$\sigma_{ef,f} \equiv \bar{\sigma}_f$ [MPa] – effective stress in fracture, according to the von Mises

K [MPa] – material strength coefficient

n [-] – strain hardening coefficient

Considering constant volume condition, relationship between strains can be described as follows:

$$d\varepsilon_1 + d\varepsilon_2 + d\varepsilon_3 = 0 \tag{7}$$

From Eq.(7) is resulting:

$-d\varepsilon_3 = d\varepsilon_1 + d\varepsilon_2$ and $d\varepsilon_3^2 = (-d\varepsilon_3)^2 = (d\varepsilon_1 + d\varepsilon_2)^2 = d\varepsilon_1^2 + 2 \cdot d\varepsilon_1 \cdot d\varepsilon_2 + d\varepsilon_2^2$

$$d\varepsilon_1^2 + d\varepsilon_2^2 + d\varepsilon_3^2 = d\varepsilon_1^2 + d\varepsilon_2^2 + (d\varepsilon_1^2 + 2 \cdot d\varepsilon_1 \cdot d\varepsilon_2 + d\varepsilon_2^2) = 2 \cdot d\varepsilon_1^2 \cdot \left(1 + \alpha + \alpha^2\right) \tag{8}$$

where:

$$\alpha = \frac{d\varepsilon_2}{d\varepsilon_1} = \frac{\varepsilon_2}{\varepsilon_1} \tag{9}$$

α [-] – constant strain ratio of material when the strain dependence is assumed to be linear.

If an Eq. (8) is appointed to an Eq. (3) consequently modified a von Mises equation of effective plastic strain increment depends only on two strains and it is in a following form:

$$d\bar{\varepsilon} = \sqrt{\frac{2}{3}} \cdot \sqrt{d\varepsilon_1^2 + d\varepsilon_2^2 + d\varepsilon_3^2} = -\frac{2 \cdot d\varepsilon_1}{\sqrt{3}} \cdot \sqrt{1 + \alpha + \alpha^2} \tag{10}$$

The some other stress-strain criteria are described in references [3,4,5]. According to the works [6], that should be considered as most precise stress-strain criteria derived by authors Cockcroft-Latham and Oyane et al. for all sample shapes [7,8].

The Cockcroft-Latham (CL) criterion is described by a formula:

$$\int_0^{\bar{\varepsilon}_f} \sigma_{2,\max} \cdot d\bar{\varepsilon} = C_2 \tag{11}$$

where:

$\sigma_{2,\max}$ [MPa] – largest principal tensile stress

The CL criterion doesn't include influence of hydrostatic stress (σ_m). The authors [9] implied that the largest principal stress (σ_2) has to be considered because the distinction between the levels of the largest principal stress and the hydrostatic stress is not very important.

The CL criterion Eq. (11) can be solved as follows:

– expressing of σ_1 or σ_2 and dε at strain ratio $\alpha = (d\varepsilon_2/d\varepsilon_1)$
– integration of stress – strain curve in interval $\bar{\varepsilon} \in \langle 0; \bar{\varepsilon}_f \rangle$

Oh et al. [10] have modified a CL criterion through normalizing of maximum principle tensile stress for uni-axial loading by the effective stress. This form was defined as a normalized CL (nCL) criterion:

$$nCL = \int_0^{\bar{\varepsilon}_f} \frac{\sigma_{2,\max}}{\bar{\sigma}} \cdot d\bar{\varepsilon} \tag{12}$$

where:

$\sigma_{2,\max}$ [MPa] – largest tensile principal stress for uni-axial loading

If power hardening Ludwig – Hollomon formula Eq. (5) is considered, the Eq. (12) can be defined in a following form:

$$nCL = \int_0^{\bar{\varepsilon}_f} \frac{\sigma_{2,\max}}{\bar{\sigma}} \cdot d\bar{\varepsilon} = \frac{\sigma_{2,\max}}{\bar{\sigma}} \int_0^{\bar{\varepsilon}_f} d\bar{\varepsilon} = \frac{\sigma_{2,\max}}{\bar{\sigma}_f} \int_0^{\bar{\varepsilon}_f} d\bar{\varepsilon} = \frac{\sigma_{2,\max}}{K \cdot \bar{\varepsilon}_f^n} \cdot \bar{\varepsilon} = \frac{\sigma_{2,\max}}{K \cdot \bar{\varepsilon}_f^{n-1}} \tag{13}$$

The authors [11] defined a solution of Eq. (11) by formula as follows:

$$C_2 = \frac{(1 + 2 \cdot \alpha)}{\sqrt{3 \cdot (1 + \alpha + \alpha^2)}} \cdot \frac{K \cdot \bar{\varepsilon}_f^{(n+1)}}{(n+1)} \cdot \frac{\varepsilon_1}{|\varepsilon_1|} \tag{14}$$

For better graphical visualization of space with fracture formation, the authors [12] derived an equation which transformed the FFLD fracture locus to the space of the equivalent plastic strain and stress triaxiality in a form:

$$\bar{\varepsilon}_f^{'} = \frac{C_2^{'}}{\sqrt{3}} \cdot \frac{3 \cdot \eta + \sqrt{12 - 27 \cdot \eta^2}}{2 + 2 \cdot \eta \cdot \sqrt{12 - 27 \cdot \eta^2}} \tag{15}$$

resp.

$$C_2^{'} = \bar{\varepsilon}_f \cdot \sqrt{3} \cdot \frac{2 + 2 \cdot \eta \cdot \sqrt{12 - 27 \cdot \eta^2}}{3 \cdot \eta + \sqrt{12 - 27 \cdot \eta^2}} \tag{16}$$

where:

$C_2^{'}$ [-] – calibration constant which is needed to determine experimentally

$\eta = \sigma_m / \bar{\sigma}_f$ [-] – parameter of stress triaxiality

$\sigma_m = (\sigma_1 + \sigma_2)/3$[MPa] – hydrostatic pressure for cylindrical co – ordinates

(17)

All methods mentioned above can be classified as analytical mathematical methods for calculation of material fracture conditions.

The main aim of the paper is to predict a material workability. According to the physical simulation carried out through a compression test as well as numerical simulation by means of ECAR process, damage conditions were achieved. Consequently fracture criteria (FFLD, Freudenthal and Cockroft-Latham criteria) were applied to analyse the results from both simulations. Moreover, proposed equations allow to predict the material workability for ECAR process of studied aluminium PM (Powder Metallurgy) material.

2. Experimental material and methods

For the experiment, it was used an aluminium alloy with chemical composition given in the TABLE 1.

TABLE 1
Local chemical analysis of ALUMIX 321 and EN AW 6062 (wt.%)

Material	Mg	Mn	Si	Cu	Cr	Zn	Fe	Al
ALUMIX 321	0,89	0	0,53	0,26	0	0,03	0,06	98,1
AW 6062-bulk	0,8-1,2	0,15	0,4-0,8	0,15-0,4	0,04-0,14	0,25	0,7	96,5

The material marked as an ALUMIX 321 was prepared by PM (powder metallurgy) technology under the following conditions: compacting pressure 400 MPa, dewaxing at 400°C for 60 min, sintering in a vacuum at 610°C for 30 min and cooling rate 6°C/sec. The chemical composition of ALUMIX 321 is approximately identical to aluminium alloy EN AW 6062.

Stress-strain curves were drawn from low-speed compression tests carried out on cylindrical samples with height-to-diameter ratio of H_0/D_0 =10mm/10mm =1 at ambient temperature using hydraulic machine with maximal loading 1MN. The frictional conditions on the anvil – sample interface were determined by a ring compression test performed at ambient temperature. Because of different surface's state of anvils, various friction conditions (f = 0, 05, 0, 06, 0, 1) were obtained. Consequently, the test was stopped in the moment when a first crack on a sample's surface was seen. The strains were measured according to the method shown in Fig. 1.

Numerical simulations of ECAR process were carried out through a software product Deform 3D focused on a study of stress, strain, strain rate and temperature progress as well as on calculation of damage criteria in a sample during processing. Also physical simulations on ECAR equipment at ambient temperature were made. The strain calculations were performed as follows:

Axial strain:

$$\varepsilon_1 = \ln \frac{H_1}{H_0} \text{ or } \varepsilon_1 = \ln \frac{h_1}{h_0} \tag{18}$$

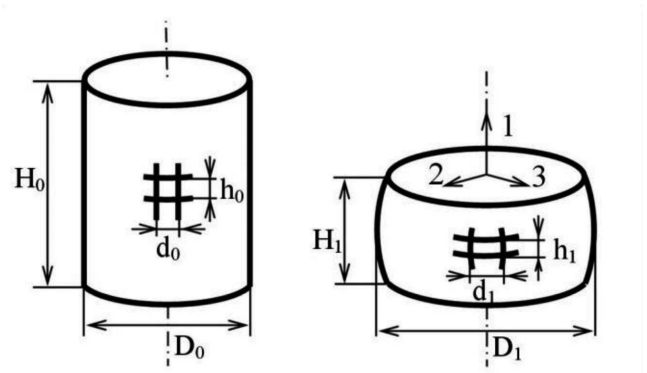

Fig. 1. The measurements of geometrical parameters for calculations of strain

Circumferential strain:

$$\varepsilon_2 = \ln \frac{D_1}{D_0} \text{ or } \varepsilon_2 = \ln \frac{d_1}{d_0} \tag{19}$$

3. Results and discussion

a) Determination of a fracture forming limit diagram (FFLD) – a compression test

The fracture criterion is based on the evaluation of strain state when fracture occurs and effective strain $\bar{\varepsilon}$ reaches a critical value $\bar{\varepsilon}_f$ i.e. $\bar{\varepsilon} = \bar{\varepsilon}_f$.

The deformation curves obtained from a compression tests under different friction conditions are given at Fig. 2.

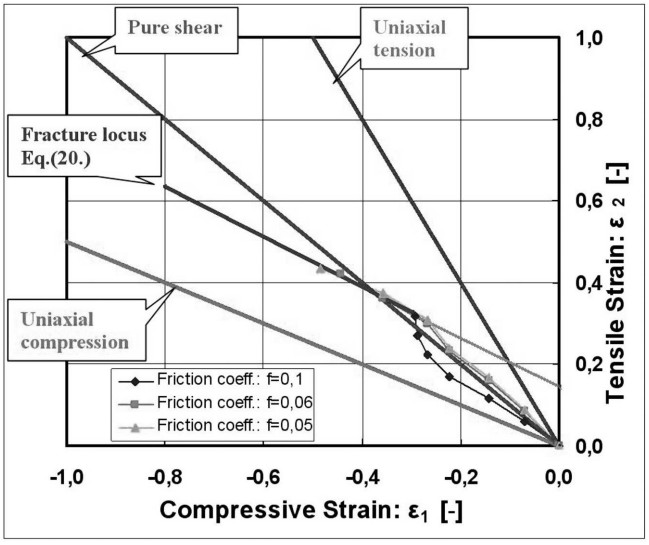

Fig. 2. Fracture forming limit diagram

The end values given on strain curves represent a fracture on a sample's free surface. If end values on strain curves were approximated by a linear function then following regression equations were derived as fracture criteria (I_{YX} =0,98):

$$\varepsilon_{2,f} = 0,14373 - 0,61446 \cdot \varepsilon_{1,f} \tag{20}$$

$$\varepsilon_{1,f} = 0,234 - 1,6275 \cdot \varepsilon_{2,f} \tag{21}$$

The values which are involved in intervals $\varepsilon_1 \in (0;\ \varepsilon_{1,f}\ )$ and $\varepsilon_2 \in (0;\ \varepsilon_{2,f})$ can be defined as a set of points without fracture

occurrence. If strain values are involved in intervals $\varepsilon_1 \in <\varepsilon_{1,f}$;∞) and $\varepsilon_2 \in <\varepsilon_{2,f}$;∞) i.e. lying on or above a line which illustrates a fracture criterion, these values can be defined as a set of points with fracture occurrence.

b) Determination of a CL criterion by expressing σ_1 or σ_2 and dε – a compression test

The effective strain on a sample in a moment when a fracture occurs can be calculated for cylindrical co-ordinates as follows:

– from von Mises equation:

$$\bar{\varepsilon}_f = \sqrt{\frac{2}{3}} \cdot \sqrt{\varepsilon_{1,f}^2 + \varepsilon_{2,f}^2} \tag{22}$$

– from modified von Mises equation by a strain ratio α:

$$\bar{\varepsilon}_f = -\frac{2 \cdot \varepsilon_{1,f}}{\sqrt{3}} \cdot \sqrt{1 + \alpha + \alpha^2} \tag{23}$$

where:

$$\alpha = \frac{\varepsilon_{2,f}}{\varepsilon_{1,f}} \tag{24}$$

$\varepsilon_{1,f}$ and $\varepsilon_{2,f}$ [-] – logarithmic principal strains at cracks initiation on a free surface

The strains $\varepsilon_{1,f}$ and $\varepsilon_{2,f}$ should be determined as follows:

– through measurement of network changes (before upsetting and in a moment of cracks initiation)
– through a calculation from regression Eqs. (20, 21)

If the Eqs. (20, 21) are substituted by the Eq. (22) consequently a formula describing a fracture criterion is in a following form:

$$\bar{\varepsilon}_f = \sqrt{\frac{2}{3}} \cdot \sqrt{\varepsilon_{1,f}^2 + \varepsilon_{2,f}^2} = \sqrt{\frac{2}{3}} \cdot \sqrt{\varepsilon_{1,f}^2 + (0,14373 - 0,61446 \cdot \varepsilon_{1,f})^2} \tag{25}$$

Also, when the Eqs. (20, 21) are substituted by the Eq. (24) consequently a strain ratio formula will be in a form:

$$\alpha = \frac{\varepsilon_{2,f}}{\varepsilon_{1,f}} = \frac{0,14373 - 0,61446 \cdot \varepsilon_{1,f}}{0,234 - 1,6275 \cdot \varepsilon_{2,f}} \tag{26}$$

A summary of the values calculated by different equations for friction coefficient f = 0,1 is given in TABLE 2.

According to the TABLE 2, high conformity between calculated data using different equations and data obtained from processing of a network (which covers a sample surface) is seen. In general, a CL criterion defines a relationship between stress and strain. Therefore it is necessary to search this relation using a mathematical theory of plastic deformations. Stresses emerging on a free sample surface during a compression can be defined by a Levi-Mises equation considering increments of plastic strain to stress in an isotropic material. These equations expressed in cylindrical co-ordinates and also with application Ludwig – Hollomon law have following forms:

$$\sigma_1 = -\frac{\bar{\sigma}}{\sqrt{3}} \cdot \frac{(\alpha + 2)}{\sqrt{\alpha^2 + \alpha + 1}} = -\frac{K \cdot \bar{\varepsilon}^n}{\sqrt{3}} \cdot \frac{(\alpha + 2)}{\sqrt{\alpha^2 + \alpha + 1}} \tag{27}$$

$$\sigma_2 = -\frac{\bar{\sigma}}{\sqrt{3}} \cdot \frac{(2\alpha + 1)}{\sqrt{\alpha^2 + \alpha + 1}} = -\frac{K \cdot \bar{\varepsilon}^n}{\sqrt{3}} \cdot \frac{(2\alpha + 1)}{\sqrt{\alpha^2 + \alpha + 1}} \tag{28}$$

$$\text{If } \beta = \frac{\sigma_2}{\sigma_1} \text{ so } \beta = \frac{\sigma_2}{\sigma_1} = \frac{2\alpha + 1}{\alpha + 2} \tag{29}$$

TABLE 2

An overview of values calculated by different equations for friction coefficient f = 0,1

No.	Description	$\varepsilon_{1,f}$	$\varepsilon_{2,f}$	α	$\bar{\varepsilon}_f$	Δ[%]
1.	Strains from network measurement	-0,293	0,317			-
2.	Strains Eq. (20): $\varepsilon_{2,f} = 0,14373 - 0,61446 \cdot \varepsilon_{1,f}$	(-0,293)	0,324			2,2
3.	Strains Eq. (21): $\varepsilon_{1,f} = 0,234 - 1,6275 \cdot \varepsilon_{2,f}$	-0,282	(0,317)			-3,8
4.	Coeff. from measured strains Eq. (24): $\alpha = \varepsilon_{2,f} / \varepsilon_{1,f}$	(-0,293)	(0,317)	-1,082		-
5.	Coeff. from Eq. (26): $\alpha = (0,14373 - 0,61446 \cdot \varepsilon_{1,f}) / (0,234 - 1,6275 \cdot \varepsilon_{2,f})$	(-0,282)	(0,324)	-1,148		5,7
6.	Effective strain- von Mises Eq. (22): $\bar{\varepsilon}_f = \sqrt{2/3} \cdot \sqrt{\varepsilon_{1,f}^2 + \varepsilon_{2,f}^2}$	(-0,293)	(0,317)		0,352	-
7.	Effective strain Eq. (23) $+\alpha \rightarrow$Eq. (24): $\bar{\varepsilon}_f = -((2 \cdot \varepsilon_{1,f}) / \sqrt{3}) \cdot \sqrt{1 + \alpha + \alpha^2}$	(-0,293)		(-1,082)	0,353	0,3
8.	Effective strain Eq. (23) $+\alpha \rightarrow$Eq. (26): $\bar{\varepsilon}_f = -((2 \cdot \varepsilon_{1,f}) / \sqrt{3}) \cdot \sqrt{1 + \alpha + \alpha^2}$	(-0,293)		(-1,148)	0,366	3,8
9.	Effective strain Eq. (25): $\bar{\varepsilon}_f = \sqrt{2/3} \cdot \sqrt{\varepsilon_{1,f}^2 + (0,14373 - 0,61446 \cdot \varepsilon_{1,f})^2}$	(-0,293)			0,357	1,4

When the stress-strain curve was drawn through measuring of geometrical parameter's changes on cylindrical samples during compression test and consequently measured values were approximated using a Ludwig – Hollomon equation as a regression, then derived regression equation is given in TABLE 3.

TABLE 3
Regression of Ludwig – Hollomon equations for a friction condition f=0,1

Friction coeff. [-]	Regression equation: $\bar{\sigma} = K \cdot \bar{\varepsilon}^n$ [MPa]	Point co-ordinates for a first crack $(\bar{\varepsilon}_f;\bar{\sigma}_f)$ [- ; MPa]	I_{yx}	Eq.(No.)
f=0,1	$\bar{\sigma} = 299 \cdot \bar{\varepsilon}^{0,19}$	(0,352; 245,3)	0,98	(30)

Validity of regression equation depends on a last point in co-ordinates $(\bar{\varepsilon}_f;\bar{\sigma}_f)$ of the curve in which the first crack on a sample surface was seen.

Considering cylindrical co-ordinate (σ_3 =0), von Mises equation for effective fracture stress will be in a following form:

$$\bar{\sigma}_f = \frac{1}{\sqrt{2}} \cdot \sqrt{\left(\sigma_{1,f} - \sigma_{2,f}\right)^2 + \left(\sigma_{2,f} - \sigma_{3,f}\right)^2 + \left(\sigma_{1,f} - \sigma_{3,f}\right)^2} = \sqrt{\sigma_{1,f}^2 + \sigma_{2,f}^2 - \sigma_{1,f} \cdot \sigma_{2,f}} \tag{30}$$

When $\bar{\sigma}_f$is substituted by Ludwig – Hollomon Eq. (30) and appointed to Eq. (31), then a relationship between principal stresses and effective fracture strain will be in a form:

$$\bar{\varepsilon}_f = \left[\frac{1}{K} \cdot \sqrt{\sigma_{1,f}^2 + \sigma_{2,f}^2 - \sigma_{1,f} \cdot \sigma_{2,f}}\right]^{1/n} \tag{31}$$

TABLE 4
The calculated values of essential parameters

No.	Description	f=0,1	Eq.(No.)
1.	$\bar{\varepsilon}_f$ [-]	0,352	(22)
2.	α [-]	-1,0819	(24)
3.	$\sigma_{1,f}$ [MPa]	-124,6	(27)
4.	$\sigma_{2,f}$ [MPa]	157,9	(28)
5.	σ_m [MPa]	11,1	(17)
6.	$\bar{\sigma}_f$ [MPa]	245,2	(31)
7.	β [-]	-1,2677	(29)
8.	Freudenthal [MPa]	72,5	(6)
8.	CL [MPa]	55,6	(11)
9.	CL [MPa]	46,7	(14)
10.	nCL [-]	0,23	(13)

The Eq. (32) describing a dependence between principal stresses and effective strain in a fracture point is one of way how to define a damage state. As mentioned above, the authors [12] derived an Eqs. (15, 16) and consequently they transformed the FFLD fracture locus to the space of the equivalent plastic fracture strain and stress to a triaxial conditions. For solution of Eqs. (15, 16), it is necessary to derive a calibration constant $C_2^{'}$ which was experimentally found for ALUMIX 321 and its numerical value is 0, 43. The steps describing calculations of numerical values are given in TABLE 4.

The graphical interpretation of Eq. (13) considering measured values for different friction conditions (f=0,1, 0,06, 0,05) are given in Fig. 3.

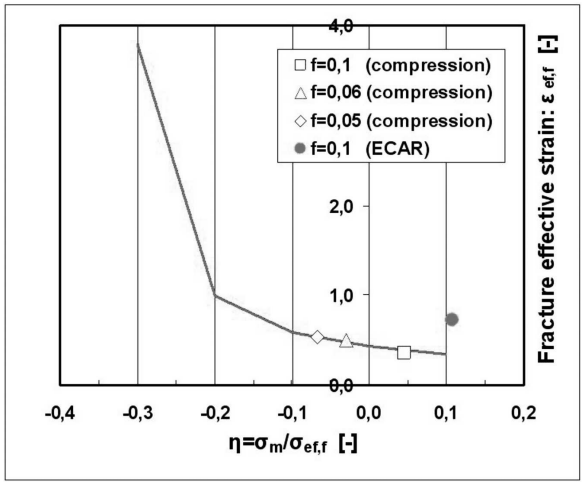

Fig. 3. Comparison of prediction CL model with experimental values

All of the values lying on and above a curve describe the states of material fracture. The measured points from compression test realized under different friction conditions are extremely well with fracture CL model.

c) Determination of CL damage criterion ECAR process – numerical simulation

Damage criteria (CL and nCL) obtained from numerical simulations carried out in a software Deform 3D for first ECAR pass are shown in Fig. 4 and Fig. 5.

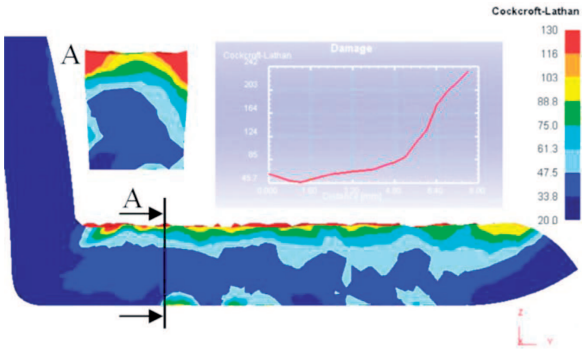

Fig. 4. CL criterion for 1st ECAR pass

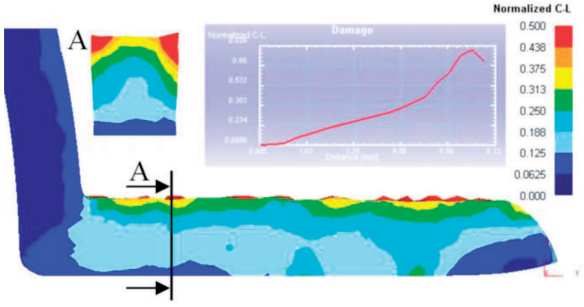

Fig. 5. nCL criterion for 1st ECAR pass

More informations related to the ECAR simulation are given in [13]. As CL and nCL values achieved from numerical simulations have not a predicative ability focused on their fracture value, a next step was calculated these damage criteria by analytic methods which were described in a previous part. The calculated damage criteria for ECAR processing with friction coefficient f = 0, 1 are given in TABLE 5.

TABLE 5
Damage criteria calculated by analytical methods for first ECAR pass

Eq. (11)	Eq. (6)	Eq. (13)
CL [MPa]	Freudenthal	nCL [-]
154	177	0,53

According to the damage criteria calculated using analytical methods, it is possible to define the fracture's start in graphical dependences achieved from numerical simulation. From graphical dependences which are given in Fig. 4 and Fig. 5, it is obvious that cracks start to emerge on upper corners of sample's cross section in the moment when the damage criteria achieve the values calculated by analytical methods given in TABLE 5.

The central sample part of sample cross section is less sensitive to a fracture creation. All the numerical methods which were used show that a material ALUMIX 321 prepared by PM technology has limited workability and after processing by one ECAR pass, fractures on upper corners of sample's cross section occur. Similar results in terms of limited workability were observed on identical material which was processed by ECAP and ECAP-BP technology as is given in literature [14, 15]. If results from numerical simulations were inserted to a prediction of the CL model (Fig. 3) then it is seen an evident deviation of ECAR point from a CL model what defines an occurrence of fractures on samples.

4. Conclusions

According to the literature review, physical and numerical simulations carried out on aluminium alloy ALUMIX 321 prepared by PM, following conclusions should be defined:

– to determine the friction coefficients, stress – strain curves in different friction conditions and fracture criteria derived through analytical mathematical methods, physical simulations were being performed

– workability criteria resulting from compression test were defined as follows:

- FFL diagram based on evaluation of strain state when fracture occurs
- criteria based on analytical mathematical methods (Freudenthal, CL, nCL)
- transformation of the FFLD fracture locus to the space of the equivalent plastic fracture strain and stress triaxiality

– calculation of workability criteria by numerical simulation through a Deform 3D provides only their numerical values which cannot be used for prediction of fracture formations

– for evaluation of numerical values obtained from numerical simulations, it is necessary to perform physical simulations on real samples with identical material characteristics

– according to the physical simulations, a method for prediction of fracture formations in a real material processed in ECAR conditions was developed which allows to predict fracture formations during numerical simulation

– according to the physical and numerical simulations, PM material ALUMIX 321 processed by one ECAR pass will be failed by ductile fracture.

Acknowledgements

This work was realized within the frame of the Operational Program Research and Development: "The centre of competence for industrial research and development in the field of light metals and composites", project code ITMS: 26220220154 and financially supported by a European Regional Development Fund.

REFERENCES

[1] A.G. Atkins, Y.W. Mai, Elastic and Plastic Fracture, Wiley, New York 1985.
[2] F.A. Freudenthal, The Inelastic Behaviour of Solids, Wiley, New York 1950.
[3] A. Venugopal Rao, N. Ramakrishnan, R.K. Kumar, J. Mater. Process. Technol. **142**, 29 (2003).
[4] J. Landre, A. Pertence, P.R. Cetlin, J.M.C. Rodrigues, P.A.F. Martins, Finite Elem. Anal. Des. **39**, 175 (2003).
[5] G. Ryzinska, Acta Metall. Slovaca **18**, (2012) (in press).
[6] B.P.P.A. Gouveia, J.M.C. Rodrigues, P.A.F. Martins, J. Mater. Process. Technol. **101**, 52 (2000).
[7] M.G. Cockroft, D.J. Latham, J. Inst. Met. **96**, 33 (1968).
[8] M. Oyane, T. Sato, K. Okimoto, S. Shima, J. Mech. Work. Technol. **4**, 65 (1980).
[9] B.P.P.A. Gouveia, J.M.C. Rodrigues, P.A.F. Martins, Int. J. Mech. Sci. **38**, 361 (1996).
[10] S.I. Oh, C.C. Chen, S. Kobayashi, Trans. ASME, J. Eng. Indus. **101**, 36 (1979).
[11] A.S. Wifi, N. El-Abbasi, A. Abdel-Hamid, A study of workability criteria in bulk forming processes, in: S.K. Ghosh, M. Predeleanu (Ed.), Materials Processing Defects, Elsevier, 333 (1995).
[12] T. Wierzbicki, Y. Bao, Y.W. Lee, Y. Bai, Int. J. Mech. Sci. **47**, 719 (2005).
[13] M. Kvačkaj, T. Kvačkaj, A. Kováčová, R. Kočiško, J. Bacsó, Acta Metall. Slovaca **16**, 84 (2010).
[14] J. Bidulská, R. Kočiško, R. Bidulský, M. Actis Grande, T. Donič, M. Martikán, Acta Metall. Slovaca **16**, 4 (2010).
[15] R. Bidulský, J. Bidulská, M. Actis Grande, High Temp. Mater. Processes **28**, 337 (2009).

Received: 20 January 2013.